Sensitivity analysis methods for mitigating uncertainty in engineering system design

Sensitivity Analysis Methods for Mitigating Uncertainty in Engineering System Design

Qinxian Chelsea Curran*[1], Douglas Allaire[2], and Karen Willcox[1]

[1]Department of Aeronautics and Astronautics, Massachusetts Institute of Technology, Cambridge, MA 02139

[2]Department of Mechanical Engineering, Texas A&M University, College Station, TX 77843

Abstract

For many engineering systems, current design methodologies do not adequately quantify and manage uncertainty as it arises during the design process, which can lead to unacceptable risks, increases in programmatic cost, and schedule overruns. This paper develops new sensitivity analysis methods that can be used to better understand and mitigate the effects of uncertainty in system design. In particular, a new entropy-based sensitivity analysis methodology is introduced which apportions output uncertainty into contributions due to not only the variance of input factors and their interactions, but also to features of the underlying probability distributions that are related to distribution shape and extent. Local sensitivity analysis techniques are also presented which provide computationally inexpensive estimates of the change in output uncertainty resulting from design modifications. The proposed methods are demonstrated on an engineering example to show how they can be used in the design context to systematically manage uncertainty budgets — which specify the allowable level of uncertainty for a system — by helping to identify design alternatives, evaluate tradeoffs between available options, and guide decisions regarding the allocation of resources.

1 Introduction

The rise of complexity in engineering systems over the years has been a well-documented trend [Kim and Wilemon, 2003; Brown and Eremenko, 2006; Warwick, 2010; Becz et al., 2010]. The challenges associated with complexity in system design include ensuring the accuracy of computational models to simulate and predict system behavior, committing considerable time and resources to conduct experimentation and testing, and managing large, globally-distributed design teams. This complexity in modern engineering systems poses a significant challenge to designers and decision-makers. Early-stage design decisions are critical because they lock in many aspects of the system performance and cost. Yet these decisions are made when uncertainty is greatest, making it difficult to guarantee a robust and reliable system. In light of these challenges, current system design methodologies are no longer adequate for identifying and addressing performance, cost, and schedule risks as they emerge during the design process. Instead, innovative uncertainty quantification methods are needed in order to rigorously identify and mitigate various sources of uncertainty associated with simulation models, numerical algorithms, experiments, and predicted quantities of interest [Smith, 2014].

This work proposes an approach in which we represent the design process as a stochastic process model. In doing so, we create a mathematical model for quantification and management of uncertainty that casts system design as a Bayesian estimation problem. Feedback of system sensitivities guides both design decisions and resource allocation decisions. In this way, the design process becomes a series of decisions targeted to achieve system specifications while also managing the associated uncertainty. The key steps of our Bayesian system design framework are shown in Figure 1. Here, a system is defined as a collection of interrelated elements that interact with one another to achieve a common purpose [NASA, 2007; Papalambros and Wilde,

*Author to whom all correspondence should be addressed (e-mail: qche@mit.edu)

This is the author manuscript accepted for publication and has undergone full peer review but has not been through the copyediting, typesetting, pagination and proofreading process, which may lead to differences between this version and the Version of Record. Please cite this article as doi: 10.1002/sys.21422

2000]. This could be a physical entity, such as a vehicle, or an abstract concept, such as a software program or procedure. The system, whatever its form, must satisfy a set of targets to be deemed successful. These targets refer to functional requirements that dictate the system's performance and level of uncertainty, as well as additional constraints that stipulate conditions such as budget and time. From these system targets, a designer must define a discrete set of parameters that map the targets to aspects of the design that can be manipulated to satisfy those requirements [Suh, 1990]. These design parameters can include quantities that define the system itself, such as individual component dimensions, as well as information describing procedures for the system's manufacture, operation, and maintenance [Deyst, 2002]. In addition to the design parameters, there are also variables that describe features of the system's performance that are of interest to the designer. We refer to these variables generically as quantities of interest (QOI). Quantities of interest are typically evaluated indirectly as functions of the design parameters. Once the design parameters and the QOI have been specified, subsequent efforts in the design process typically involve the conception of various design alternatives, the analysis of those options using computer models and simulation tools, and the development and testing of prototypes to verify performance [NASA, 2007; Hazelrigg, 1996; Braha and Maimon, 1997; Thomke and Bell, 2001; Browning et al., 2002]. This iterative procedure is represented in the Bayesian system design framework by the *design feedback* loop in Figure 1, which terminates when a feasible design is achieved that satisfies all system targets [Suh, 1990; Nightingale, 2000].

For most realistic engineering systems, the design process is made more difficult by the presence of non-deterministic features that contribute to uncertainties in the system [Oberkampf et al., 2002]. This paper presents novel sensitivity analysis methods that can be used in system design to identify the key drivers of uncertainty, enumerate design options, and evaluate tradeoffs in the context of resource allocation decisions for uncertainty mitigation. The information provided by our methods enable both an *uncertainty feedback* loop, which is used to update requirements and parameter distributions in our stochastic process model of the design process, as well as a *resource allocation* loop used to determine how to best use resources to achieve design goals.

Our approach focuses on two measures of uncertainty in the QOI: complexity and risk. These measures and their computational quantification were developed as part of the Defense Advanced Research Projects Agency's (DARPA) Adaptive Vehicle Make (AVM) initiative, which seeks to streamline the systems engineering process and enable the development of newer, better defense vehicles more quickly and at lower cost [Belfiore, 2012; Eremenko, 2013]. To date, the methods developed in our work have been tested on a first principles-based infantry fighting vehicle model [He et al., 2012] and an infantry fighting vehicle bond graph model developed by the Vanderbilt University Institute for Software Integrated Systems [Lattmann et al., 2012; Allaire et al., 2012] to demonstrate their utility for designing and testing vehicle components. In this paper, we apply our methods to the design and analysis of a high-pass filter circuit, which is another use case of the DARPA-AVM program.

The rest of the paper proceeds as follows. Section 2 frames the context of the paper, introduces complexity and risk as metrics for quantifying uncertainty, and provides a discussion of existing sensitivity analysis methods. Section 3 describes the development of two new sensitivity analysis methodologies: an uncertainty decomposition approach centered on the apportionment of output entropy power into contributions due to the shape and extent of the input factors and their interactions, and a set of local sensitivity analysis techniques that can be used to estimate changes in complexity and risk associated with a design update. Section 4 uses a circuit example to demonstrate the applicability of the proposed sensitivity analysis methods, as well as introduce the idea of an uncertainty budget and describe its relevance to system design. In particular, sensitivity information is combined with cost and uncertainty budgets to identify specific design options that satisfy system constraints, visualize tradeoffs in the design space, and inform decisions regarding the allocation of resources aimed at enhancing robustness and reliability. Finally, Section 5 summarizes the key contributions of the paper and highlights some areas of future work.

2 Background

This section provides an overview of several topics relevant to the work presented in this paper: the quantification of uncertainty in engineering system design (Section 2.1), the implications of uncertainty for system robustness and reliability (Section 2.2), and existing methods for performing sensitivity analysis (Section 2.3).

2.1 Characterizing Uncertainty

Uncertainty in engineering systems can come in many flavors; for example, it can be broadly categorized as *epistemic*, owing to insufficient or imperfect knowledge, or *aleatory*, which arises from natural randomness and is therefore irreducible [Smith, 2014; Roy and Oberkampf, 2011; Oberkampf et al., 2002; Ang and Tang, 2007]. Another classification of uncertainty focuses on the underlying source of the uncertainty in the design process, and includes parameter uncertainty, parametric variability, residual variability, observation error, model inadequacy, and code uncertainty [Kennedy and O'Hagan, 2001].[1] Although we concern ourselves mainly with parameter uncertainty in this paper, we note that the methods presented herein are intended to be general enough to describe any of the aforementioned types of uncertainty, provided that they can be described probabilistically.

In this work, we focus on the development of methods to understand and mitigate the effects of uncertainty during the intermediate stages of system design, where requirements, design parameters, and quantities of interest have already been defined, but no feasible design has yet been realized. Design parameters are variables that relate the requirements in the functional domain to aspects of the design in the physical domain that can be manipulated to satisfy those requirements [Suh, 1990]. We assume that all design parameters within a system are independent, and denote them using the $m \times 1$ vector $\mathbf{x} = [x_1, x_2, \ldots, x_m]^\intercal$, where x_i is the i^{th} design parameter among a total of m design parameters. Quantities of interest are used to characterize aspects of the system's performance that are of interest to the designer, and are typically evaluated as functions of the design parameters using available models and analysis tools. We represent them using the $n \times 1$ vector $\mathbf{y} = [y_1, y_2, \ldots, y_n]^\intercal$, where y_j is the j^{th} QOI out of a total of n. For simplicity, we will assume that there already exist models and tools (may be black-box) with which to evaluate the QOI of a system from the design parameters. We express this relationship as:

$$\mathbf{y} = g(\mathbf{x}), \tag{1}$$

where $g : \mathbb{R}^m \to \mathbb{R}^n$ denotes the mapping from design parameters to QOI. For the j^{th} QOI y_j, this mapping is given by:

$$y_j = g_j(\mathbf{x}), \tag{2}$$

where $g_j : \mathbb{R}^m \to \mathbb{R}^1$, and $j = 1, 2, \ldots, n$.

To characterize the propagation of uncertainty within a system, we employ continuous random variables to represent design parameters and QOI, and model the time evolution of design as a stochastic process whose outcome is governed by some probability distribution. We use $\mathbf{X} = [X_1, X_2, \ldots, X_m]^\intercal$ and $\mathbf{Y} = [Y_1, Y_2, \ldots, Y_n]^\intercal$ to denote vectors of random variables that correspond to the entries of $\mathbf{x}$ and $\mathbf{y}$, respectively.

Using Monte Carlo (MC) simulation, we generate numerous estimates of each QOI, from which a probability density can be estimated. To quantify the uncertainty associated with a particular QOI Y, we employ the metrics of complexity and risk. For complexity, we use the definition that it is the potential of a system to exhibit unexpected behavior in the QOI, whether detrimental or not [Allaire et al., 2012]. The quantitative metric associated with this definition is exponential entropy [Campbell, 1966], which is the exponential of the differential entropy of Y:

$$C(Y) = \exp[h(Y)] = \exp\left[-\int_{\mathbb{Y}} f_Y(y) \log f_Y(y)\, \mathrm{d}y\right]. \tag{3}$$

A related quantity to exponential entropy is entropy power [Shannon, 1948], which is proportional to the square of exponential entropy, and denoted by $N(Y)$:

$$N(Y) = \frac{\exp[2h(Y)]}{2\pi e} = \frac{C(Y)^2}{2\pi e}. \tag{4}$$

[1] According to Kennedy and O'Hagan [2001], parameter uncertainty results from not knowing the true values of the inputs to a model, parametric variability relates to unspecified conditions in the model inputs or parameters, residual variability is due to the inherently unpredictable or stochastic nature of the system, observation error refers to uncertainty associated with actual observations or measurements, model inadequacy is due to the insufficiency of any model to exactly predict reality, and code uncertainty arises from not knowing the output of a model given a particular set of inputs until the code is run.

Whereas $C(Y)$ is a measure of *intrinsic extent* and has the same units as Y,[2] $N(Y)$ exhibits properties of variance and has the same units as Y^2. This provides an appealing analogy for the relationship between standard deviation and variance to that between exponential entropy and entropy power.

In this work, we define risk as the probability that a system incurs an undesirable outcome, such as violating a requirement or constraint. Suppose that a QOI is subject to the requirement that it must be greater than or equal to a specified value r. In this case, risk corresponds to the probability that the random variable Y takes on a value less than r, given by:

$$P(Y < r) = \int_{-\infty}^{r} f_Y(y)\,\mathrm{d}y. \tag{5}$$

This notion of risk is illustrated in Figure 2, where $P(Y < r)$ corresponds to the area of the shaded region in which the requirement is not met.[3]

2.2 Designing for Robustness and Reliability

Uncertainty in engineering design is closely related to the *robustness* and *reliability* of the resulting systems. Here, we use the definition that robustness is "the property of systems that enables them to survive unforeseen or unusual circumstances" [Knoll and Vogel, 2009]. That is to say, to improve a system's robustness is to make it less susceptible to exhibit unexpected behavior in the presence of a wide range of stochastic elements [Karl, 2013; Creveling et al., 2003]. Reliability, on the other hand, describes a system's "probability of success in satisfying some performance criterion" [Haldar and Mahadevan, 2000], and is closely tied to system safety [Karl, 2013].[4] Under this definition, reliability is the complement of risk, which instead describes the probability of failure.

Graphically, we illustrate the distinction between design for robustness and design for reliability in Figure 2, in which our estimate of a QOI Y is updated from the red probability density to the blue. The dashed line $y = r$ represents a performance criterion below which the design is deemed unacceptable; the area of the shaded region corresponds to $P(Y < r)$. Figure 2(a) shows a constant scaling of $f_Y(y)$ with no change in the mean value, whereas Figure 2(b) depicts a constant shift (horizontal translation) of $f_Y(y)$ with no change in the standard deviation. Both activities have direct implications for the uncertainty associated with Y. In practice, improvements in robustness and reliability can occur concurrently, as depicted in Figure 2(c). In this paper, however, we will treat them as distinct activities in order to investigate how robustness and reliability are related to our proposed measures of uncertainty — complexity and risk — as well as how sensitivity analysis can be used to predict changes in these quantities.

2.3 Variance-Based Sensitivity Analysis

In the context of engineering system design, sensitivity analysis allows us to better understand the effects of uncertainty in order to make well-informed decisions aimed at uncertainty reduction. For example, it can be used to study how "variation in the output of a model ... can be apportioned, qualitatively or quantitatively, to different sources of variation, and how the given model depends upon the information fed into it" [Saltelli et al., 2000]. Existing sensitivity analysis approaches typically use variance as a measure of uncertainty.

[2]The intrinsic extent of a random variable Y is always less than or equal to the range of Y (i.e., the "true" extent) [Campbell, 1966]. One interpretation of intrinsic extent is as "the equivalent side length of the smallest set that contains most of the probability" [Cover and Thomas, 1991]. That is to say, whereas range gives the length of the interval (potentially infinite) that contains all possible values y for which $Y = y$, the intrinsic extent represents the (finite) extent of Y once the various values of y have been weighted by their probability of occurrence. In the case where Y is a uniform random variable, intrinsic extent and range are equivalent.

[3]The probability of failure can also be defined as $P(Y > r)$ in the case that the QOI must not exceed r.

[4]Alternate definitions of reliability also ascribe an element of time. For example, reliability is sometimes described as the probability of failure within a given interval of time [Kapur and Lamberson, 1977], or the expected life of a product or process, typically measured by the mean time to failure or the mean time between failures [Creveling et al., 2003]. We will not address the temporal aspect of reliability in this paper.

2.3.1 Global Sensitivity Analysis

In variance-based global sensitivity analysis (GSA), variability in a model's output (i.e., a system's QOI) is apportioned into contributions from each of the factors (i.e., the design parameters), as well as their interactions. This notion is illustrated in Figure 3.

A common approach for conducting GSA is the Sobol' method, which utilizes MC simulation to characterize the propagation of uncertainty [Homma and Saltelli, 1996; Sobol', 1993, 2001, 2003]. The Sobol' method is based on high-dimensional model representation (HDMR), which decomposes a function $g(\mathbf{X})$ into the following sum:

$$g(\mathbf{X}) = g_0 + \sum_i g_i(X_i) + \sum_{i<j} g_{ij}(X_i, X_j) + \ldots + g_{12\ldots m}(X_1, X_2, \ldots, X_m), \tag{6}$$

where g_0 is a constant, $g_i(X_i)$ is a function of X_i only, $g_{ij}(X_i, X_j)$ is a function of X_i and X_j only, etc. Although (6) is not a unique representation of $g(\mathbf{X})$, it can be made unique by enforcing the following constraints:

$$\int_0^1 g_{i_1,\ldots,i_s}(X_{i_1}, \ldots, X_{i_s})\, \mathrm{d}x_k = 0, \qquad \forall \quad \begin{matrix} k = i_1, \ldots, i_s, \\ s = 1, \ldots, m. \end{matrix} \tag{7}$$

In the above equation, the indices $i_1, \ldots, i_s$ represent all sets of s integers that satisfy $1 \leq i_1 < \ldots < i_s \leq m$. That is, for $s = 1$, the constraint given by (7) applies to all sub-functions $g_i(X_i)$ in (6); for $s = 2$, the constraint applies to all sub-functions $g_{ij}(X_i, X_j)$ with $i < j$ in (6), etc. Furthermore, in (7) we have defined all factors $X_{i_1}, \ldots, X_{i_s}$ on the interval $[0, 1]$; this is merely for simplicity of presentation, and not a requirement of the Sobol' method. With the sub-functions $g_{i_1,\ldots,i_s}(X_{i_1}, \ldots, X_{i_s})$ now uniquely specified, we refer to (6) as the analysis of variances high-dimensional model representation (ANOVA-HDMR) of $g(\mathbf{X})$.

Alternatively, we can write the ANOVA-HDMR in terms of the random variables Y, Z_i, $Z_{ij}, \ldots, Z_{12\ldots m}$ to denote the outputs of the original function and various sub-functions, respectively. That is, we let $Y = g(\mathbf{X})$ and $Z_{i_1,\ldots,i_s} = g_{i_1,\ldots,i_s}(X_{i_1}, \ldots, X_{i_s})$, where the indices $i_1, \ldots, i_s$ represent all sets of s integers that satisfy $1 \leq i_1 < \ldots < i_s \leq m$. The ANOVA-HDMR can thus be expressed as:

$$Y = g_0 + \sum_i Z_i + \sum_{i<j} Z_{ij} + \ldots + Z_{12\ldots m}. \tag{8}$$

Since all sub-functions in (6) are orthogonal and zero-mean, $Z_i, Z_{ij}, \ldots, Z_{12\ldots m}$ (henceforth termed *auxiliary random variables*) are all uncorrelated. Accordingly, the variance of Y is the sum of the partial variances of Z_1 through Z_m and their higher-order interactions:

$$\mathrm{var}\,(Y) = \sum_i \mathrm{var}\,(Z_i) + \sum_{i<j} \mathrm{var}\,(Z_{ij}) + \ldots + \mathrm{var}\,(Z_{12\ldots m}). \tag{9}$$

Normalizing by $\mathrm{var}\,(Y)$, the proportional contribution to $\mathrm{var}\,(Y)$ from each of the auxiliary random variables is given by:

$$1 = \sum_i \frac{\mathrm{var}\,(Z_i)}{\mathrm{var}\,(Y)} + \sum_{i<j} \frac{\mathrm{var}\,(Z_{ij})}{\mathrm{var}\,(Y)} + \ldots + \frac{\mathrm{var}\,(Z_{12\ldots m})}{\mathrm{var}\,(Y)}. \tag{10}$$

A key result in GSA is the estimation of the main effect sensitivity index (MSI) for each factor. For a system modeled by (1), the MSI of the i^{th} factor, denoted by S_i, represents the expected relative reduction in the variance of Y if the true value of X_i is learned (i.e., the variance of X_i is reduced to zero):

$$S_i = \frac{\mathrm{var}\,(Y) - \mathbb{E}\left[\mathrm{var}\,(Y|X_i)\right]}{\mathrm{var}\,(Y)} = \frac{\mathrm{var}\,(Z_i)}{\mathrm{var}\,(Y)}. \tag{11}$$

For a particular model, $\sum_{i=1}^m S_i \leq 1$; deviation from unity reflects the magnitude of the interaction effects. The various factors of a model can be ranked according to MSI in a factor prioritization setting to determine the factors that, once their true values are known, would result in the greatest expected reduction in output variability; these correspond to the factors with the largest values of S_i.

2.3.2 Distributional Sensitivity Analysis

A related approach to global sensitivity analysis is distributional sensitivity analysis (DSA), which can be used to evaluate the expected reduction in output variance when the variance of an input factor is only partially reduced [Allaire, 2009; Allaire and Willcox, 2012]. Instead of assuming that input variability can be decreased to zero through further research and improved knowledge, DSA instead treats the portion of a factor's variance that can be reduced as a random variable. Therefore, DSA may be more appropriate than GSA for the prioritization of efforts aimed at uncertainty reduction, as it could convey for which input(s) directed research will yield the greatest return. Assuming no interactions between the inputs, in many cases DSA can be implemented without running additional MC simulations by reusing samples from a previous Sobol'-based GSA.

Letting X_i^o be the random variable corresponding to the original distribution for factor i, and X_i' be the random variable whose distribution represents the uncertainty in that factor after some design modification, the ratio of remaining (irreducible) variance to initial variance for factor i is defined by the quantity δ:

$$\delta = \frac{\text{var}\,(X_i')}{\text{var}\,(X_i^o)}. \tag{12}$$

When we do not know the true value of δ, we treat it as a uniform random variable on the interval $[0, 1]$. Whereas GSA computes for each factor X_i the main effect sensitivity index S_i, the analogous quantity in DSA is $\text{adjS}_i(\delta)$, the adjusted main effect sensitivity index of X_i given that it is known that only $100(1-\delta)\%$ of its variance can be reduced.[5]

3 Methodology

Building upon existing sensitivity analysis approaches, we present two new contributions in this section. First, we extend the ideas of variance-based global sensitivity analysis to develop an analogous methodology for entropy-based sensitivity analysis in Section 3.1. In Section 3.2, we develop local sensitivity analysis techniques that linearize a system about the current design to enable the estimation of uncertainty as well as the identification and evaluation of design options in subsequent iterations. Later, in Section 4, we will discuss how these sensitivity analysis methods can be used in the context of an uncertainty budget to evaluate design options and guide the allocation of resources.

3.1 Entropy-Based Sensitivity Analysis

In addition to variance-based sensitivity analysis, work has also been done in the development of methods for global and regional sensitivity analysis using information entropy as a measure of uncertainty. One such method uses the Kullback-Leibler (K-L) divergence,[6] or relative entropy, to quantify the distance between two probability distributions [Liu et al., 2006]. These distributions, represented by the random variables Y^o and Y', correspond to estimates of the QOI before and after some factor X_i has been fixed at a particular value (e.g., its mean). The K-L divergence between Y^o and Y' serves to quantify the impact of the factor that has been fixed; that is to say, the larger the value of $D_{KL}(Y^o||Y')$, the more substantial the contribution of factor i to uncertainty in the QOI.

[5] The main effect sensitivity indices computed from GSA correspond to the case where $\delta = 0$.

[6] For arbitrary continuous random variables W_1 and W_2, the K-L divergence from W_1 to W_2 is defined as [Kullback and Leibler, 1951]:

$$\begin{aligned} D_{KL}(W_1||W_2) &= \int_{-\infty}^{\infty} f_{W_1}(w) \log \frac{f_{W_1}(w)}{f_{W_2}(w)}\, \mathrm{d}w \\ &= \int_{-\infty}^{\infty} f_{W_1}(w) \log f_{W_1}(w)\, \mathrm{d}w - \int_{-\infty}^{\infty} f_{W_1}(w) \log f_{w_2}(w)\, \mathrm{d}w \\ &= -h(W_1) + h(W_1, W_2). \end{aligned} \tag{13}$$

The above relationship shows that $D_{KL}(W_1||W_2)$ is equal to the sum of two terms: the negative of the differential entropy $h(W_1)$ plus the cross entropy $h(W_1, W_2)$ between W_1 and W_2.

The relative entropy-based approach can be used to perform both global and regional sensitivity analysis by simply adjusting the limits of integration, and is suitable for distributions where variance is not a good measure of uncertainty (e.g., bimodal or skewed distributions). However, the sensitivity analysis results can vary depending on where a particular factor is fixed on its domain. Furthermore, the K-L divergence is not normalized and does not have physical meaning — it can be used to rank factors, but does not have a proportion interpretation such as shown in Figure 3 for variance-based sensitivity indices. Taking these issues into consideration, we present a novel entropy-based sensitivity analysis methodology which builds upon the concept of uncertainty decomposition from variance-based GSA. For this, we use entropy power as the basis for our sensitivity analysis approach, recalling from (4) that entropy power is proportional to the square of exponential entropy.

3.1.1 Entropy Power Decomposition

We desire to derive a similar decomposition expression to (10) for $N(Y)$, the entropy power of the QOI. Although there is no general relationship between entropy power and variance [Mukherjee and Ratnaparkhi, 1986; Ebrahimi et al., 1999], for a given random variable, entropy power is always less than or equal to variance, with equality in the case where the random variable is Gaussian. Therefore, we seek to relate the disparity between variance and entropy power to the random variable's degree of non-Gaussianity, quantified using the K-L divergence. To do this, we define an *equivalent Gaussian distribution*, which is a Gaussian random variable with the same mean and variance as the original random variable. For an arbitrary random variable W, we denote its equivalent Gaussian distribution using the superscript G and define it as $W^G \sim \mathcal{N}(\mu_W, \sigma_W)$, where μ_W and σ_W represent the mean and standard deviation of W, respectively.

We compute the K-L divergence between each random variable in (8) and its equivalent Gaussian distribution to obtain $D_{KL}(Y||Y^G)$, $D_{KL}(Z_1||Z_1^G)$, $D_{KL}(Z_2||Z_2^G)$, etc. This allows us to write the following sum, which we shall refer to as the *entropy power decomposition*, which relates the entropy power and non-Gaussianity of the QOI to the corresponding quantities for the auxiliary random variables:

$$\begin{aligned} N(Y)\exp[2D_{KL}(Y||Y^G)] = &\sum_i N(Z_i)\exp[2D_{KL}(Z_i||Z_i^G)] \\ &+ \sum_{i<j} N(Z_{ij})\exp[2D_{KL}(Z_{ij}||Z_{ij}^G)] \\ &+ \ldots + N(Z_{12\ldots m})\exp[2D_{KL}(Z_{12\ldots m}||Z_{12\ldots m}^G)]. \end{aligned} \tag{14}$$

The derivation of (14) is provided in Appendix I, and is based on the observation that for any arbitrary random variable W, $\mathrm{var}\,(W) = N(W)\exp[2D_{KL}(W||W^G)]$. The implication of the entropy power decomposition is that the variance of each of Y and Z_i, Z_{ij}, $\ldots$, $Z_{12\ldots m}$ is equal to the product of the variable's entropy power and an exponential term, where the argument of the exponential is two times the K-L divergence of the variable with respect to its equivalent Gaussian distribution. Thus, it follows that (9) and (14) are equivalent up to a multiplicative factor of $2\pi e$.

A key aspect in the derivation of the entropy power decomposition is that we have not made any additional assumptions about the underlying distributions of Y or the auxiliary random variables beyond the requirements dictated by the ANOVA-HDMR: finite variance and uncorrelated auxiliary random variables.[7] Having obtained analogous expressions for the decomposition of output variance and entropy power into comprising terms, we can normalize (14) to establish a similar interpretation in terms of proportional contributions from the input factors and their interactions:

$$\begin{aligned} 1 = &\sum_i \frac{N(Z_i)}{N(Y)}\frac{\exp[2D_{KL}(Z_i||Z_i^G)]}{\exp[2D_{KL}(Y||Y^G)]} + \sum_{i<j}\frac{N(Z_{ij})}{N(Y)}\frac{\exp[2D_{KL}(Z_{ij}||Z_{ij}^G)]}{\exp[2D_{KL}(Y||Y^G)]} \\ &+ \ldots + \frac{N(Z_{12\ldots m})}{N(Y)}\frac{\exp[2D_{KL}(Z_{12\ldots m}||Z_{12\ldots m}^G)]}{\exp[2D_{KL}(Y||Y^G)]}. \end{aligned} \tag{15}$$

[7] We emphasize the distinction between uncorrelated random variables Z_i and Z_j ($i \neq j$), for which the variance of the sum is equal to the sum of the variances (i.e., $\mathrm{var}\,(Z_i + Z_j) = \mathrm{var}\,(Z_i) + \mathrm{var}\,(Z_j)$), and independent random variables X_i and X_j, for which the joint probability density $f_{X_i,X_j}(x_i, x_j)$ is equal to the product of the marginal densities $f_{X_i}(x_i)$ and $f_{X_j}(x_j)$.

In (15), the proportion of output uncertainty directly due to X_i consists of two parts: one that is the ratio of the entropy power of Z_i to that of Y, and one that is the ratio of the exponential of twice the K-L divergence from Z_i to Z_i^G to the analogous quantity for Y. Recalling that exponential entropy — proportional to the square root of entropy power — measures the intrinsic extent of a random variable, we conclude that the first ratio is directly influenced by the intrinsic extent of X_i (and thus Z_i). On the other hand, the second ratio is directly related to the non-Gaussianity of X_i (and thus Z_i). To illustrate this, we introduce the entropy power sensitivity indices η_i and ζ_i, defined as:

$$\eta_i = \frac{N(Z_i)}{N(Y)}, \tag{16}$$

$$\zeta_i = \frac{\exp[2D_{KL}(Z_i||Z_i^G)]}{\exp[2D_{KL}(Y||Y^G)]}. \tag{17}$$

The above expressions correspond to the main effect indices for factor i; analogous expressions can also be derived for the higher-order interactions. Due to the equivalence of (10) and (15), η_i and ζ_i are related to the variance-based main effect sensitivity index S_i as follows:

$$S_i = \eta_i \zeta_i. \tag{18}$$

Substituting η_i and ζ_i into (15) gives:

$$1 = \eta_1\zeta_1 + \eta_2\zeta_2 + \ldots + \eta_{12\ldots m}\zeta_{12\ldots m}. \tag{19}$$

The proportion of output uncertainty due to each factor directly can be divided into an intrinsic extent effect characterized by the sensitivity index η_i, which is related to complexity, and a non-Gaussianity effect characterized by the sensitivity index ζ_i, which is related to distribution shape. The product of the two effects equals the MSI of the factor. This allows us to associate (15) with the uncertainty apportionment notion depicted in Figure 3.

Note that in the previous paragraph we used the phrase "due to each factor directly" instead of "due to each factor alone." This choice of wording reflects the fact that a change in any auxiliary random variable Z_i can affect both the intrinsic extent and the non-Gaussianity of Y. Thus, the quantities $N(Y)$ and $D_{KL}(Y||Y^G)$ are impacted, which indirectly affects the indices η_j and ζ_j of all other auxiliary variables Z_j where $i \neq j$. Because it is usually difficult to determine *a priori* how changing Z_i would modify $N(Y)$ and $D_{KL}(Y||Y^G)$, it is typically impractical to decouple the direct and indirect effects that alterations to Z_i would impose on the entropy power decomposition. Despite this limitation, the entropy power sensitivity indices still reveal useful information about how the spread and distribution shape of each input factor contribute to uncertainty in the output quantity of interest.

3.1.2 The Effect of Distribution Shape

The K-L divergence between Z_i and its equivalent Gaussian distribution is invariant to design updates that result in a shift in mean or scaling of $f_{Z_i}(z)$ by a constant, as shown in Figures 2(b) and 2(a), respectively. The first case is easy to intuit, since by definition Z_i and Z_i^G have the same mean. To see the latter, we examine the case where $Z_i' = \alpha Z_i^o$.[8] It is easy to show that $h(Z_i') = h(Z_i^o) + \log\alpha$ [Cover and Thomas, 1991]. Making use of the relations $f_{Z_i'}(z) = \frac{1}{\alpha} f_{Z_i^o}(\frac{z}{\alpha})$ and $\xi = \frac{z}{\alpha}$, we can compute the cross entropy $h(Z_i', Z_i'^G)$ as follows:

$$\begin{aligned}
h(Z_i', Z_i'^G) &= -\int_{-\infty}^{\infty} \frac{1}{\alpha} f_{Z_i^o}(\frac{z}{\alpha}) \log\left[\frac{1}{\alpha} f_{Z_i^{oG}}(\frac{z}{\alpha})\right] \mathrm{d}z \\
&= -\int_{-\infty}^{\infty} \frac{1}{\alpha} f_{Z_i^o}(\xi) \log\left[\frac{1}{\alpha} f_{Z_i^{oG}}(\xi)\right] \alpha \,\mathrm{d}\xi \\
&= -\int_{-\infty}^{\infty} f_{Z_i^o}(\xi) \log f_{Z_i^{oG}}(\xi) \,\mathrm{d}\xi + \log\alpha \int_{-\infty}^{\infty} f_{Z_i^o}(\xi) \,\mathrm{d}\xi \\
&= h(Z_i^o, Z_i^{oG}) + \log\alpha.
\end{aligned} \tag{20}$$

[8] Technically, Figure 2(a) shows a multiplicative scaling case where Z_i^o has a mean of zero. For nonzero values of $\mu_{Z_i^o}$, we can introduce a constant shift of $\Delta\mu = -\mu_{Z_i^o}$ to recenter Z_i' at the origin, such that $Z_i' = \alpha(Z_i^o - \mu_{Z_i^o})$ and $f_{Z_i'}(z) = \frac{1}{\alpha} f_{Z_i^o}(\frac{z}{\alpha} + \mu_{Z_i^o})$. However, note that this shift is for illustrative purposes only, as the derivation in (20) does not require Z_i^o and Z_i' to be zero-mean.

Combining (13) and (20), we obtain:

$$D_{KL}(Z_i'||Z_i'^G) = D_{KL}(Z_i^o||Z_i^{oG}). \tag{21}$$

The above result implies that the non-Gaussianity of a random variable remains constant if its underlying distribution maintains the same shape to within a multiplicative constant. For example, if Z_i^o and Z_i' are both uniform random variables, but Z_i' has a narrower distribution, the fundamental shape of the probability density is not affected, and therefore the two variables have the same degree of non-Gaussianity. However, if Z_i^o and Z_i' are both triangular random variables, but one has a symmetric distribution and the other a skewed distribution, then Z_i^o and Z_i' have differing levels of non-Gaussianity. This is because the underlying distribution shape has changed, even though both variables are of the triangular family. Finally, as a note of caution, we reiterate that even if a design activity has no effect on $D_{KL}(Z_i||Z_i^G)$, ζ_i can still be impacted indirectly through changes to $D_{KL}(Y||Y^G)$ imparted by other factors.

Since it is a measure of distance, the K-L divergence is always non-negative. As a measure of non-Gaussianity, $D_{KL}(Z_i||Z_i^G)$ equals zero if and only if Z_i itself is Gaussian, and is positive otherwise. This implies that in (15), $\exp[2D_{KL}(Z_i||Z_i^G)] \geq 1$. However, ζ_i can be greater than, less than, or equal to one, depending on the relative magnitude of the numerator and denominator in (17). That is to say, ζ_i indicates whether an auxiliary random variable Z_i is less Gaussian ($\zeta_i > 1$), more Gaussian ($\zeta_i < 1$), or equally as Gaussian ($\zeta_i = 1$) as the QOI Y. Next, we consider the three cases separately for a system modeled by $Y = X_1 + X_2$, where X_1 and X_2 are either uniform or Gaussian random variables. Note that this system does not contain interaction effects, and thus $Z_1 = X_1$, $Z_2 = X_2$, and $Z_{12} = 0$.

For the first case, we let X_1 and X_2 be independent and identically distributed uniform random variables on the interval $[-0.5, 0.5]$ (Figure 4(a)). The sum $Y = X_1 + X_2$ has a symmetric triangular distribution on the interval $[-1, 1]$. In this case, both ζ_1 and ζ_2 exceed one (Figure 5(a)), as moving from the design parameters to the QOI corresponds to an increase in Gaussianity. Figure 4(b) shows an example where X_1 is uniform and X_2 is Gaussian, resulting in a distribution for Y that is more Gaussian than X_1 but less Gaussian than X_2. In this case, the corresponding indices for non-Gaussianity are $\zeta_1 > 1$ and $\zeta_2 < 1$ (Figure 5(b)). Finally, if both X_1 and X_2 are Gaussian, then $X_1 + X_2$ is also Gaussian (Figure 4(c)), and $\zeta_1 = \zeta_2 = 1$ (Figure 5(c)).

3.2 Local Sensitivity Analysis

In the context of engineering design, once the key drivers of uncertainty in a system have been identified, the task of uncertainty mitigation centers on making decisions regarding design modifications in the subsequent iteration [NASA, 2007; Suh, 1990; Takeda et al., 1990]. Such decisions often relate to the allocation of resources in order to improve one or more aspects of the design. Resources can be allocated to a variety of different activities — for example, to direct future research, to conduct experiments, to improve physical and simulation-based modeling capabilities, or to invest in superior hardware or additional personnel.

In the following setions, we develop local sensitivity analysis techniques for estimating complexity and risk, which can inform how those quantities are affected by small changes in the mean or standard deviation of a system's design parameters or QOI, and thus guide decisions regarding the allocation of resources.

3.2.1 Relationship to Variance-Based Sensitivity Indices

Sensitivity indices from variance-based GSA and DSA can help designers understand the potential for reduction in output variance resulting from design activities that decrease variability in the inputs. Revisiting Figures 2(a) and 2(b), we consider the separate cases of a constant shift that alters the mean versus a multiplicative scaling that shrinks the standard deviation. These design activities have direct implications for system robustness and reliability.

To evaluate the local sensitivity of complexity and risk with respect to updates that perturb the mean or standard deviation of the QOI, we compute the partial derivative of $C(Y)$ and $P(Y < r)$ with respect to μ_Y and σ_Y. The partial derivatives can then be linearized about the current design to predict the change in complexity (ΔC) or risk (ΔP) associated with a perturbation in mean ($\Delta\mu_Y$) or standard deviation ($\Delta\sigma_Y$). These expressions are derived in He et al. [2012] and listed in (22)–(29).

Sensitivity of $C(Y)$ with respect to μ_Y and σ_Y

Partial derivatives

$$\frac{\partial C(Y)}{\partial \mu_Y} = 0 \quad (22) \qquad \frac{\partial C(Y)}{\partial \sigma_Y} = \frac{C(Y)}{\sigma_Y} \quad (23)$$

Local approximations

$$\Delta C(Y) = 0 \quad (24) \qquad \Delta C \approx \frac{\Delta \sigma_Y}{\sigma_Y} C(Y) \quad (25)$$

Sensitivity of $P(Y < r)$ with respect to μ_Y and σ_Y

Partial derivatives

$$\frac{\partial P(Y < r)}{\partial \mu_Y} = -f_Y(r) \quad (26) \qquad \frac{\partial P(Y < r)}{\partial \sigma_Y} = \frac{(\mu_Y - r)}{\sigma_Y} f_Y(r) \quad (27)$$

Local approximations

$$\Delta P \approx -\Delta \mu_Y f_Y(r) \quad (28) \qquad \Delta P \approx \frac{\Delta \sigma_Y}{\sigma_Y} (\mu_Y - r) f_Y(r) \quad (29)$$

From (22), we see that perturbations in μ_Y do not affect complexity. This is unsurprising, as we know that $C(Y)$ contains no information about the expected value of Y. From (23), we see that the sensitivity of complexity to σ_Y is a constant, and simply equals the ratio of $C(Y)$ to σ_Y. Since both $C(Y)$ and σ_Y are non-negative, this implies that as a local approximation, reducing standard deviation also reduces complexity.

More interestingly, (26) and (27) show that the sensitivity of risk to both μ_Y and σ_Y is proportional to the probability density of Y evaluated at the requirement r. Since $f_Y(y) \geq 0$ for all values of y, this implies that the sign of $\Delta \mu_Y$ or $\mu_Y - r$ determines whether risk is increased or decreased (see (28) and (29)). Figure 6 helps to illustrate this point for (29), where a reduction in standard deviation can alter risk in either direction, depending on the relative locations of r and μ_Y.

Another contribution of this paper, presented below, is the derivation of expressions that relate the local uncertainty approximations shown in (25) and (29) to sensitivity indices computed from variance-based GSA and DSA and entropy power sensitivity analysis. In this derivation, we let Y^o and Y' represent initial and new estimates of the QOI (the red and blue densities in Figure 6, respectively) corresponding to a design activity that reduces variance (and thus standard deviation). Similarly, we let $\text{var}\,(Y^o)$ and $\text{var}\,(Y')$ represent the variance of the QOI before and after the update, respectively. If the activity is one that results in learning the true value of factor i, then we know from (11) that:

$$\text{var}\,(Y') = \text{var}\,(Y^o) - S_i \text{var}\,(Y^o). \quad (30)$$

The ratio of $\text{var}\,(Y')$ to $\text{var}\,(Y^o)$ is given by:

$$\frac{\text{var}\,(Y')}{\text{var}\,(Y^o)} = 1 - S_i. \quad (31)$$

We can relate the above ratio to the quantity $\Delta \sigma_Y / \sigma_Y$ from (25) and (29):

$$\begin{aligned} \frac{\Delta \sigma_Y}{\sigma_Y} &= \frac{\sqrt{\text{var}\,(Y')} - \sqrt{\text{var}\,(Y^o)}}{\sqrt{\text{var}\,(Y^o)}} \\ &= \sqrt{\frac{\text{var}\,(Y')}{\text{var}\,(Y^o)}} - 1 \\ &= \sqrt{1 - S_i} - 1. \end{aligned} \quad (32)$$

This allows us to rewrite (25) and (29) as:

$$\Delta C \approx (\sqrt{1 - S_i} - 1) C(Y), \quad (33)$$

$$\Delta P \approx (\sqrt{1 - S_i} - 1)(\mu_Y - r) f_Y(r), \quad (34)$$

noting that $C(Y)$, μ_Y, and $f_Y(r)$ in the above expressions refer to the complexity, mean, and probability density (evaluated at r) of the QOI for the initial design. Finally, if the design activity is instead one that reduces the variance of factor i by $100(1-\delta)\%$, then (30) can be modified to:

$$\text{var}\,(Y') = \text{var}\,(Y^o) - \text{adj}S_i(\delta)\text{var}\,(Y^o), \tag{35}$$

and we can similarly substitute $\text{adj}S_i(\delta)$ for S_i in (33) and (34). Since both S_i and $\text{adj}S_i(\delta)$ can only assume values in the interval $[0,1]$, the above local approximations imply that a decrease in variance is concurrent with a reduction in complexity, as well as in risk if $\mu_Y - r > 0$. While an attractive result, these relations are simply local approximations and should not be generalized.

3.2.2 Local Approximation of Risk

In order to use sensitivity information about the QOI to update the design, it is necessary to translate this information into tangible actions for modifying the design parameters. For this, we extend (26) and (27) to compute the sensitivity of risk to perturbations in the mean or standard deviation of the design parameters.

We define the vectors $\mu_{\mathbf{X}} = [\mu_{X_1}, \mu_{X_2}, \ldots, \mu_{X_m}]^\intercal$ and $\sigma_{\mathbf{X}} = [\sigma_{X_1}, \sigma_{X_2}, \ldots, \sigma_{X_m}]^\intercal$, which consist of the mean and standard deviation estimates of the entries of $\mathbf{X}$, respectively. Using the chain rule, the partial derivative of $P(Y < r)$ with respect to μ_{X_i} is given by:

$$\frac{\partial P(Y<r)}{\partial \mu_{X_i}} = \frac{\partial P(Y<r)}{\partial \mu_Y}\frac{\partial \mu_Y}{\partial \mu_{X_i}}. \tag{36}$$

To estimate $\partial\mu_Y/\partial\mu_{X_i}$, we use (2) and make the following approximation for μ_Y:

$$\mu_Y = \mathbb{E}\,[g(\mathbf{X})] \approx g(\mathbb{E}\,[\mathbf{X}]) = g(\mu_{\mathbf{X}}). \tag{37}$$

This approximation is exact if $g(\mathbf{X})$ is linear. Therefore, we have:

$$\frac{\partial \mu_Y}{\partial \mu_{X_i}} \approx \frac{\partial g(\mu_{\mathbf{X}})}{\partial X_i}. \tag{38}$$

Combining (26), (36), and (38), we obtain:

$$\frac{\partial P(Y<r)}{\partial \mu_{X_i}} \approx -f_Y(r)\frac{\partial g(\mu_{\mathbf{X}})}{\partial X_i}, \tag{39}$$

$$\Delta P \approx -\Delta\mu_{X_i} f_Y(r)\frac{\partial g(\mu_{\mathbf{X}})}{\partial X_i}. \tag{40}$$

Similarly, the partial derivative of $P(Y < r)$ with respect to σ_{X_i} is given by:

$$\frac{\partial P(Y<r)}{\partial \sigma_{X_i}} = \frac{\partial P(Y<r)}{\partial \sigma_Y}\frac{\partial \sigma_Y}{\partial \sigma_{X_i}}. \tag{41}$$

To approximate $\partial\sigma_Y/\partial\sigma_{X_i}$, we can use results from DSA to estimate $\Delta\sigma_Y/\Delta\sigma_{X_i}$. The adjusted main effect sensitivity index $\text{adj}S_i(\delta)$ relates the expected variance remaining in Y (given by (35)) to the variance remaining in factor i (given by (12)) as δ ranges between 0 and 1, which allows us to compute $\Delta\sigma_Y/\Delta\sigma_{X_i}$ as follows:

$$\begin{aligned}\frac{\Delta\sigma_Y}{\Delta\sigma_{X_i}} &= \frac{\sqrt{\text{var}\,(Y^o) - \text{adj}S_i(\delta)\text{var}\,(Y^o)} - \sqrt{\text{var}\,(Y^o)}}{\sqrt{\delta\text{var}\,(X_i^o)} - \sqrt{\text{var}\,(X_i^o)}} \\ &= \frac{\sigma_Y(\sqrt{1-\text{adj}S_i(\delta)}-1)}{\sigma_{X_i}(\sqrt{\delta}-1)}.\end{aligned} \tag{42}$$

Thus, we can combine (27), (41) and (42) to obtain:[9]

$$\frac{\partial P(Y<r)}{\partial \sigma_{X_i}} \approx \frac{f_Y(r)(\mu_Y - r)(\sqrt{1-\text{adj}S_i(\delta)}-1)}{\sigma_{X_i}(\sqrt{\delta}-1)}, \tag{43}$$

$$\Delta P \approx \frac{\Delta\sigma_{X_i} f_Y(r)(\mu_Y - r)(\sqrt{1-\text{adj}S_i(\delta)}-1)}{\sigma_{X_i}(\sqrt{\delta}-1)}. \tag{44}$$

The key result of this section is that we can relate system risk to the specific changes in the design parameters. As an example, let ΔP denote the desired change in risk. Rearranging (40) and (44), we can estimate the requisite change in the mean and standard deviation of the i^{th} design parameter in order to achieve that goal. For small values of ΔP, these changes are approximated by:

$$\Delta\mu_{X_i} \approx -\frac{\Delta P}{f_Y(r)}\left[\frac{\partial g(\mu_{\mathbf{X}})}{\partial X_i}\right]^{-1}, \tag{45}$$

$$\Delta\sigma_{X_i} \approx \frac{\Delta P\,\sigma_{X_i}(\sqrt{\delta}-1)}{f_Y(r)(\mu_Y - r)(\sqrt{1-\text{adj}S_i(\delta)}-1)}. \tag{46}$$

The above expressions allow the designer to obtain a first-order estimate of the parameter adjustments needed to achieve a desired decrease in risk. They can also highlight different trends, tradeoffs, and design tensions present in the system. However, we note again that these relations are merely local approximations whose predictive accuracy cannot be guaranteed. Furthermore, they do not account for interactions among the design parameters, nor do they imply that the suggested changes in mean or standard deviation are necessarily feasible, as limitations due to physical or budgetary constraints are not accounted for. It is the responsibility of the designer to use these tools as a guideline for cost-benefit analysis of various design activities, and ultimately select the most appropriate action for risk mitigation.

3.2.3 Local Approximation of Complexity

Next, we use the results from entropy power decomposition to approximate complexity in the QOI resulting from a design update. For simplicity, we will consider a system consisting of two factors, X_1 and X_2, although the approach can be extended to higher dimensions. We let X_1^o and X_2^o denote the design parameters corresponding to the initial design, and X_1' and X_2' denote the updated estimates for those parameters after the design modification. Similarly, letting $i = 1, 2$, we write the following relations:

$$\begin{aligned} Z_i^o &= g_i(X_i^o) & Z_i' &= g_i(X_i') \\ Y^o &= g(X_1^o, X_2^o) & Y' &= g(X_1', X_2') \\ \zeta_i^o &= \frac{\exp[2D_{KL}(Z_i^o||Z_i^{oG})]}{\exp[2D_{KL}(Y^o||Y^{oG})]} & \zeta_i' &= \frac{\exp[2D_{KL}(Z_i'||Z_i'^G)]}{\exp[2D_{KL}(Y'||Y'^G)]} \end{aligned}$$

Based on (15), the entropy power of Y^o can be written as:

$$N(Y^o) = N(Z_1^o)\zeta_1^o + N(Z_2^o)\zeta_2^o + N(Z_{12}^o)\zeta_{12}^o. \tag{47}$$

For the new design, we employ the following local approximation to predict $N(Y')$, which uses the non-Gaussianity indices ζ_1^o, ζ_2^o, and ζ_{12}^o evaluated at the initial design:

$$N(Y') \approx N(Z_1')\zeta_1^o + N(Z_2')\zeta_2^o + N(Z_{12}')\zeta_{12}^o. \tag{48}$$

The relationship between each input factor and the corresponding auxiliary random variable can be obtained from the ANOVA-HDMR (computed either analytically or numerically). Thus, we are able to calculate $N(Z_1')$, $N(Z_2')$, and $N(Z_{12}')$ based on X_1', X_2', and X_{12}', which then allows us to estimate $N(Y')$

[9] While (42) is a valid statement of $\Delta\sigma_Y/\Delta\sigma_{X_i}$ for any value of $\delta \in [0, 1)$, the choice of δ can greatly affect the accuracy of the local approximation $\partial\sigma_Y/\partial\sigma_{X_i} \approx \Delta\sigma_Y/\Delta\sigma_{X_i}$, especially for small values of δ (corresponding to large reductions in factor variance), or if the relationship between var (Y') and var (X_i') is highly nonlinear.

without having to explicitly evaluate Y' using MC simulation. Finally, recognizing that entropy power is proportional to the square of complexity, we can rewrite (48) to obtain an estimate of $C(Y')$:

$$C(Y') \approx \sqrt{2\pi e[N(Z_1')\zeta_1^o + N(Z_2')\zeta_2^o + N(Z_{12}')\zeta_{12}^o]}. \tag{49}$$

The methods presented in this section allow designers to estimate complexity and risk using sensitivity information about the system, which can then inform design strategies and tradeoffs. These local approximations can be especially valuable in engineering scenarios in which direct evaluation of the QOI is computationally expensive or intractable.

4 Application and Results

In this section, we demonstrate the sensitivity analysis methods introduced in this paper on an engineering example to show how they can be used in the design context to identify uncertainty mitigation options and visualize tradeoffs between design alternatives. We also present the third contribution of this paper by introducing the notion of an uncertainty budget, which can be used in conjunction with sensitivity information to ensure constraint satisfaction and inform resource allocation decisions.

4.1 Problem Setup

Consider a high-pass filter circuit shown consisting of a resistor and a capacitor in series. The design parameters of the system are resistance (R) and capacitance (C), which have nominal values of $100\,\Omega$ and $4.7\,\mu$F, respectively. The corresponding component tolerances are $R_{\text{tol}} = \pm 10\%$ and $C_{\text{tol}} = \pm 20\%$. We select the quantity of interest of the system to be the cutoff frequency f_c, which has a nominal value of 339 Hz. To achieve the desired circuit performance, the cutoff frequency must exceed 300 Hz. A schematic of the system is shown in Figure 7.

We use the random variables X_1, X_2, and Y to represent uncertainty in R, C, and f_c, respectively. Due to stochasticity in the system, the functional requirement on the QOI will be treated as a probabilistic design target (i.e., the probability that the cutoff frequency falls below 300 Hz must not exceed a specified limit). The relationship between the design parameters and the QOI is given by:

$$Y = \frac{1}{2\pi X_1 X_2}. \tag{50}$$

We model X_1 and X_2 as uniform random variables on the intervals specified by their component tolerances, such that $X_1 \sim \mathcal{U}[a_1, b_1] = \mathcal{U}[90, 110]\,\Omega$ and $X_2 \sim \mathcal{U}[a_2, b_2] = \mathcal{U}[3.76, 5.64]\,\mu$F. Using 10,000 MC samples, the histogram of Y for the nominal design is shown in Figure 8. The corresponding uncertainty estimates are: $\text{var}\,(Y) = 2015\,\text{Hz}^2$, $C(Y) = 181$ Hz, and $P(Y < 300\,\text{Hz}) = 18.6\%$.

4.2 Identifying the Drivers of Uncertainty

Global sensitivity analysis of the R-C circuit system reveals that approximately 80% of the variance in Y can be attributed to X_2 (capacitance), and the remaining 20% to X_1 (resistance), with interactions playing a negligible role (Figure 9(a)). These results are corroborated by the entropy power sensitivity indices η_i and ζ_i shown in Figure 9(b). We see that S_i is similar to η_i for both factors, and that ζ_i is equal to or slightly greater than one. This indicates that uncertainty apportionment using variance and entropy power produce similar results. Furthermore, it reveals that Gaussianity increases in moving from the input factors to the QOI. Both types of sensitivity analysis point to prioritizing uncertainty reduction in X_2.

4.3 Cost and Uncertainty Budgets

In this work, we assume that there is a cost associated with each activity that mitigates uncertainty in the QOI; this cost can be estimated from historical data, using cost estimation relationships, or through the elicitation of expert opinion. As an illustrative example, let us consider the notional curves shown in Figure 10(a) for the R-C circuit, which depicts the cost associated with a $100(1-\delta)\%$ reduction in the

variance of X_1 or X_2. In Figure 10(b), the same information is visualized as contour lines of equal cost with respect to different proportions of variance reduction in the two factors. We observe that although reducing $\mathrm{var}\,(X_2)$ is more effective in abating output uncertainty than decreasing $\mathrm{var}\,(X_1)$, it is also more expensive to implement. Furthermore, the reduction in $\mathrm{var}\,(X_2)$ is capped at 75% (that is, 25% of the variability in X_2 is irreducible), whereas $\mathrm{var}\,(X_1)$ can be reduced by as much as 99%.

The third contribution of this paper is to establish the idea of an uncertainty budget in design and to show how the proposed sensitivity analysis methods provide a systematic way of identifying design options and uncertainty reduction activities that meet system requirements as well as satisfy budget constraints. Unlike a cost budget, which specifies the amount of resources that can be expended to improve the design, an uncertainty budget refers to the total level of uncertainty that is deemed tolerable for the system. For both the cost and uncertainty budgets, we seek to determine how much of the prescribed amount ought to be allocated to each design parameter. For the R-C circuit, we impose the following budgetary constraints:

- **Complexity:** The complexity with respect to the QOI shall not exceed 150 Hz.
- **Risk:** The probability of violating the cutoff frequency requirement shall not exceed 10%.
- **Cost:** The cost of uncertainty reduction shall not exceed 20 units of cost.

Next, we examine each constraint individually in turn to study the resulting optimal allocation. Figure 11 overlays contours of variance, complexity, and risk in the QOI (solid colored lines) with those corresponding to cost of implementation (dashed green lines). These contours allow us to consider the cost and uncertainty budgets in conjunction. We see that for a given cost, the maximum possible uncertainty reduction is achieved by decreasing the variance of both X_1 and X_2 simultaneously, rather than focusing on either factor alone. Table I lists the lowest possible uncertainty and cost estimates for the system when each of the budgetary constraints ($C(Y) \leq 150\,\mathrm{Hz}$, $P(Y < 300\,\mathrm{Hz}) \leq 10\%$, Cost ≤ 20) is in turn made active. Of the three budgets, the complexity constraint is the cheapest to satisfy; however, the resulting allocation of factor variance reduction does not satisfy the risk constraint. To ensure that risk does not exceed 10%, a minimum cost of 14.8 is required; this corresponds to a complexity of 132 Hz. Finally, a cost budget of 20 is more than adequate to guarantee that the uncertainty budgets are also satisfied. As we observe in Figures 11(b) and 11(c), the expenditure of 20 units of cost is sufficient to decrease $\mathrm{var}\,(X_2)$ by up to 67%; even without a simultaneous reduction in $\mathrm{var}\,(X_1)$, it is enough to reduce complexity and risk to acceptable levels of 125 Hz and 8%, respectively.

The results in Table I suggest that the cost and uncertainty budgets for the R-C circuit design are mutually compatible and achievable. There are a host of solutions that satisfy all three budgetary constraints, which lie within the shaded region in Figure 11(d). The main tradeoff in these solutions is between cost and risk: when both of those constraints are satisfied, the complexity budget is automatically satisfied as well. In the following section, however, we will consider the cost and uncertainty budgets alongside available design options, which can lead to different conclusions regarding their feasibility.

4.4 Identifying and Evaluating Design Alternatives

Building upon the discussion on design budgets, we next study how the nominal value and tolerance of the components in the R-C circuit trade against one another in terms of contribution to uncertainty in the QOI. This analysis enables designers to visualize strategies for uncertainty mitigation in terms of actionable items in the design space.

For each of X_1 and X_2, there are two parameters that can be modified: the nominal value of the circuit component (R or C) and the tolerance (R_{tol} or C_{tol}). We vary R and C from their nominal values by up to $\pm 20\%$, and decrease R_{tol} and C_{tol} from the initial tolerances of $\pm 10\%$ and $\pm 20\%$, respectively, down to $\pm 1\%$. Figures 12 and 13 show contour lines for complexity (left) and risk (right) for different combinations of the four quantities; a black X in each figure denotes the location of the nominal design.

From Figure 12, we see that raising either R or C lowers complexity in the QOI but also increases risk, and vice-versa; this indicates the presence of competing objectives. Figure 13 shows that when trading R_{tol} against C_{tol}, decreasing the latter is more effective for reducing both complexity and risk, which is consistent with the trends observed in Figures 11(b) and 11(c).

The colored contours in Figures 12 and 13 were generated using 10,000 MC simulations to evaluate Y at each design parameter combination. The dashed black lines correspond to local approximations obtained using local sensitivity information, and can be produced without performing additional MC simulations. In particular, the complexity approximations obtained using (49) closely match the colored contours generated from brute force MC simulation. The largest discrepancies occur in Figure 13(a) for small resistor tolerances. As for risk, although the local estimates vary in accuracy, the overall trends due to changing R, C, R_{tol}, and C_{tol} are correctly captured, especially for design parameter combinations close to the nominal design (Figures 12(b) and 13(b)). Thus, our local approximation techniques provide an easy way to visualize trends in complexity and risk and identify regions in the design space that warrant additional analysis — toward which additional MC simulations can be directed to generate more rigorous estimates of uncertainty.

Figures 12 and 13 depict tradeoffs among R, C, R_{tol}, and C_{tol} as continuous within the design space, implying infinitely many design combinations. For many engineering systems, however, the design space instead contains a discrete number of feasible options dictated by component availability. Thus, we next investigate how local sensitivity analysis results can be used to identify distinct design options.

Using the expressions from (45) and (46), we can compute the requisite change in the mean and standard deviation of X_1 and X_2 needed to achieve a desired decrease in risk. In this case, we set $\Delta P = -0.086$ so as to meet the constraint that $P(Y < 300\,\text{Hz}) \leq 10\%$. Table II lists the change in mean and standard deviation of each factor required to achieve this risk reduction as predicted using local sensitivity information, as well as the corresponding component nominal value and tolerance. Consistent with the risk contours in Figure 12(b), we see that reducing risk requires decreasing R or C. This suggests that we use a resistor with a nominal value of no more than $96.6\,\Omega$, or a capacitor with a nominal value of no more than $4.54\,\mu$F. Alternatively, we can reduce risk by using components with tighter tolerances. For the resistor, the change in the standard deviation of X_1 needed to satisfy the risk constraint is $-8.4\,\Omega$; however, initially, $\sigma_{X_1} = 5.8\,\Omega$, which implies that it is not possible to achieve the requisite risk reduction by decreasing R_{tol} alone. For the capacitor, we observe that the risk constraint can be met by decreasing the standard deviation of X_2 by $-0.17\,\mu$F, which corresponds to a component tolerance of $\pm 14.4\%$.

The local sensitivity analysis predictions point the designer to values of R, C, R_{tol}, and C_{tol} that would satisfy the uncertainty budget for risk. Consulting standard off-the-shelf resistor and capacitor values [Irwin and Nelms, 2005], we identify four design alternatives — Options A–D — which correspond most closely to the desired component specifications shown in Table II. These options are listed in Table III along with their associated estimates of variance, complexity, risk, and cost of implementation. Each option perturbs one of R, C, R_{tol}, and C_{tol} from its initial value. We assume in this analysis that it is comparatively cheaper to purchase components with different nominal values (Options A and B) than it is to acquire components with significantly tighter tolerances (Options C and D).[10] The locations of the four options within the design space are indicated in Figures 12 and 13.

Figure 14 illustrates the tradeoffs between complexity and risk for the various options. Immediately, we see that none of the options satisfies both the cost and uncertainty budgets. Options A and B fall well within the cost budget and reduce risk to virtually zero; however, they both increase complexity to unacceptable levels, and thus can be eliminated from consideration.[11] In Option C, the resistor tolerance is reduced to just $\pm 1\%$ at a cost of 13.2; yet, there is virtually no change in risk compared to the initial design. Option D appears to be the most promising choice, as it is the only one to satisfy both the complexity and risk constraints. However, it exceeds the cost budget of 20.

These results suggest that in order to meet both the cost and uncertainty budgets, the designer must either seek alternative options, or relax one or more of the constraints. In Figure 14, we see that Option D falls well within the region of acceptable uncertainty. Focusing on the top right corner of that region, we find that when $C_{\text{tol}} = \pm 12.5\%$, the system achieves $C(Y) = 150\,\text{Hz}$ and $P(Y < 300\,\text{Hz}) = 10.0\%$ at a cost of 18.3, which satisfies all design budgets. However, while this design is mathematically possible, it is not realistically feasible given limitations in component availability, as standard capacitor tolerances include $\pm 20\%$, $\pm 10\%$, $\pm 5\%$, $\pm 2\%$, and $\pm 1\%$. From this analysis, we conclude that the most promising course of

[10] Assuming that X_1 and X_2 are both uniform random variables, a decrease in R_{tol} from $\pm 10\%$ to $\pm 1\%$ in Option C corresponds to a 99% reduction in $\text{var}(X_1)$, and a decrease in C_{tol} from $\pm 20\%$ to $\pm 10\%$ in Option D corresponds to a 75% reduction in $\text{var}(X_2)$. The associated costs of implementation correspond to the rightmost red and blue points in Figure 10(a), respectively.

[11] Had we instead identified options that raised the nominal values of R and C, the result would have decreased complexity and increased risk, which is similarly undesirable.

action is to allocate resources toward improving capacitor tolerance; furthermore, we recommend increasing the cost budget so that all uncertainty targets can be satisfied using standard components.

5 Conclusions and Future Work

This paper presented new sensitivity analysis methods which can be used to better understand and mitigate the effects of uncertainty in engineering system design. First, building upon existing variance-based global sensitivity analysis, an analogous interpretation of uncertainty apportionment was derived based on entropy power. This process informed that a factor's contribution to output entropy power consists of two effects, which are related to its spread (as characterized by intrinsic extent) versus distribution shape (as characterized by non-Gaussianity). Furthermore, local sensitivity analysis techniques were developed, which can be used to predict changes in the complexity and risk of the quantities of interest resulting from various design modifications. These local approximations are particularly useful for systems whose simulation models are computationally expensive, as they can be used to identify tradeoffs and infer trends in the design space without performing additional model evaluations. Finally, the proposed techniques were demonstrated on an engineering example to showcase how they can be connected with budgets for uncertainty and cost in order to identify options for improving robustness and reliability and inform decisions regarding resource allocation.

There are a number of possible extensions to the present work; two specific areas are discussed here. The first is to reduce the computational burden associated with pseudo-random Monte Carlo simulation. The use of efficient sampling methods, such as Latin hypercube or quasi-random Monte Carlo, could be explored to decrease computational cost. In particular, it would be interesting to study how such techniques can be combined with acceptance/rejection sampling or importance sampling to enable sample reuse in distributional sensitivity analysis. Another possible avenue of future work could focus on broadening the applicability of the proposed sensitivity analysis methods to problems of higher dimensionality. Although the theory underlying the methodologies can be extended to higher dimensions, implementation issues often hinder their use in practice. For example, density estimation — upon which entropy estimation is prefaced — is typically straightforward in 1-D; for higher dimensions, however, it becomes much more challenging, or even downright intractable. It is expected that advancements in the area of high-dimensional density estimation will allow the proposed sensitivity analysis methods to be applied to larger classes of engineering problems.

Acknowledgments

The authors gratefully acknowledge support from the International Design Centre at the Singapore University of Technology and Design, the DARPA META program through AFRL Contract Number FA8650-10-C-7083 and Vanderbilt University Contract Number VU-DSR #21807-S7, the National Science Foundation Graduate Research Fellowship Program, and the Zonta International Amelia Earhart Fellowship Program.

Appendix I

In this section, we derive the entropy power decomposition presented in (14) and reproduced below:

$$\begin{aligned} N(Y)\exp[2D_{KL}(Y||Y^G)] = &\sum_i N(Z_i)\exp[2D_{KL}(Z_i||Z_i^G)] \\ &+ \sum_{i<j} N(Z_{ij})\exp[2D_{KL}(Z_{ij}||Z_{ij}^G)] \\ &+ \ldots + N(Z_{12\ldots m})\exp[2D_{KL}(Z_{12\ldots m}||Z_{12\ldots m}^G)]. \end{aligned}$$

For simplicity, we shall consider a system consisting of only two input factors ($m = 2$), although the results can be generalized to higher dimensions. For such a system, the ANOVA-HDMR representation and variance decomposition (from (8) and (9), respectively) reduce to:

$$Y = g_0 + Z_1 + Z_2 + Z_{12}, \tag{51}$$

$$\mathrm{var}\,(Y) = \mathrm{var}\,(Z_1) + \mathrm{var}\,(Z_2) + \mathrm{var}\,(Z_{12}). \tag{52}$$

The auxiliary random variables Z_1, Z_2, and Z_{12} are uncorrelated, although not necessarily independent.[12] For this two-factor system, the distributions of the equivalent Gaussian random variables and the corresponding probability densities are:

$$Z_1^G \sim \mathcal{N}(\mu_{Z_1}, \sigma_{Z_1}) \qquad f_{Z_1^G}(z) = \frac{1}{\sqrt{2\pi\sigma_{Z_1}^2}} \exp\left[\frac{-(z-\mu_{Z_1})^2}{2\sigma_{Z_1}^2}\right]$$

$$Z_2^G \sim \mathcal{N}(\mu_{Z_2}, \sigma_{Z_2}) \qquad f_{Z_2^G}(z) = \frac{1}{\sqrt{2\pi\sigma_{Z_2}^2}} \exp\left[\frac{-(z-\mu_{Z_2})^2}{2\sigma_{Z_2}^2}\right]$$

$$Z_{12}^G \sim \mathcal{N}(\mu_{Z_{12}}, \sigma_{Z_{12}}) \qquad f_{Z_{12}^G}(z) = \frac{1}{\sqrt{2\pi\sigma_{Z_{12}}^2}} \exp\left[\frac{-(z-\mu_{Z_{12}})^2}{2\sigma_{Z_{12}}^2}\right]$$

$$Y^G \sim \mathcal{N}(\mu_Y, \sigma_Y) \qquad f_{Y^G}(z) = \frac{1}{\sqrt{2\pi\sigma_Y^2}} \exp\left[\frac{-(z-\mu_Y)^2}{2\sigma_Y^2}\right]$$

To verify the entropy power decomposition, we need to show that:

$$\exp[2h(Y,Y^G)] = \exp[2h(Z_1,Z_1^G)] + \exp[2h(Z_2,Z_2^G)] + \exp[2h(Z_{12},Z_{12}^G)], \tag{53}$$

where $h(Z_1, Z_1^G)$ represents the cross entropy between Z_1 and its equivalent Gaussian random variable Z_1^G (and likewise for Y, Z_2, and Z_{12}). By definition, $h(Z_1, Z_1^G)$ is computed as:

$$\begin{aligned} h(Z_1,Z_1^G) &= -\int_{-\infty}^{\infty} f_{Z_1}(z)\log f_{Z_1^G}(z)\,\mathrm{d}z \\ &= -\int_{-\infty}^{\infty} f_{Z_1}(z)\log\left\{\frac{1}{\sqrt{2\pi\sigma_{Z_1}^2}}\exp\left[\frac{-(z-\mu_{Z_1})^2}{2\sigma_{Z_1}^2}\right]\right\}\mathrm{d}z \\ &= -\int_{-\infty}^{\infty} f_{Z_1}(z)\log\left[\frac{1}{\sqrt{2\pi\sigma_{Z_1}^2}}\right]\mathrm{d}z - \int_{-\infty}^{\infty} f_{Z_1}(z)\log\left\{\exp\left[\frac{-(z-\mu_{Z_1})^2}{2\sigma_{Z_1}^2}\right]\right\}\mathrm{d}z \\ &= \log\sqrt{2\pi\sigma_{Z_1}^2}\int_{-\infty}^{\infty} f_{Z_1}(z)\,\mathrm{d}z + \frac{1}{2\sigma_{Z_1}^2}\int_{-\infty}^{\infty}(z-\mu_{Z_1})^2 f_{Z_1}(z)\,\mathrm{d}z. \end{aligned} \tag{54}$$

[12] Since Z_{12} is a function of both X_1 and X_2, it is necessarily dependent on both Z_1 and Z_2, which are respectively functions of X_1 and X_2 alone. However, Z_1 and Z_2 are independent, due to our assumption of design parameter independence.

Noting that $\int_{-\infty}^{\infty} f_{Z_1}(z)\,\mathrm{d}z = 1$ and $\int_{-\infty}^{\infty} (z-\mu_{Z_1})^2 f_{Z_1}(z)\,\mathrm{d}z = \sigma_{Z_1}^2$, (54) simplifies to:

$$h(Z_1, Z_1^G) = \log\sqrt{2\pi\sigma_{Z_1}^2} + \frac{1}{2}. \tag{55}$$

Multiplying both sides by two and taking the exponential, we get:

$$\exp[2h(Z_1, Z_1^G)] = \exp\left[2\log\sqrt{2\pi\sigma_{Z_1}^2} + 2\left(\frac{1}{2}\right)\right] = \exp\left[\log(2\pi\sigma_{Z_1}^2) + 1\right] = 2\pi e\sigma_{Z_1}^2. \tag{56}$$

Similarly, the other terms of (53) are given by:

$$\exp[2h(Z_2, Z_2^G)] = 2\pi e\sigma_{Z_2}^2, \tag{57}$$
$$\exp[2h(Z_{12}, Z_{12}^G)] = 2\pi e\sigma_{Z_{12}}^2, \tag{58}$$
$$\exp[2h(Y, Y^G)] = 2\pi e\sigma_Y^2. \tag{59}$$

Substituting (56)–(59) into (53), we obtain:

$$2\pi e\sigma_Y^2 = 2\pi e\sigma_{Z_1}^2 + 2\pi e\sigma_{Z_2}^2 + 2\pi e\sigma_{Z_{12}}^2, \tag{60}$$
$$\sigma_Y^2 = \sigma_{Z_1}^2 + \sigma_{Z_2}^2 + \sigma_{Z_{12}}^2. \tag{61}$$

We have already established that (61) is true, as it is equivalent to (52). We conclude therefore that (53) also holds true. Using (13) to relate cross entropy to differential entropy and K-L divergence, we can express (53) as follows:

$$\begin{aligned}\exp[2h(Y) + 2D_{KL}(Y||Y^G)] = {} & \exp[2h(Z_1) + 2D_{KL}(Z_1||Z_1^G)] \\ & + \exp[2h(Z_2) + 2D_{KL}(Z_2||Z_2^G)] \\ & + \exp[2h(Z_{12}) + 2D_{KL}(Z_{12}||Z_{12}^G)].\end{aligned} \tag{62}$$

Using (4), we can rewrite (62) in terms of $N(Y)$:

$$\begin{aligned}(2\pi e)N(Y)\exp[2D_{KL}(Y||Y^G)] = {} & (2\pi e)N(Z_1)\exp[2D_{KL}(Z_1||Z_1^G)] \\ & + (2\pi e)N(Z_2)\exp[2D_{KL}(Z_2||Z_2^G)] \\ & + (2\pi e)N(Z_{12})\exp[2D_{KL}(Z_{12}||Z_{12}^G)].\end{aligned} \tag{63}$$

Dividing both sides by $2\pi e$, the result becomes:

$$\begin{aligned}N(Y)\exp[2D_{KL}(Y||Y^G)] = {} & N(Z_1)\exp[2D_{KL}(Z_1||Z_1^G)] \\ & + N(Z_2)\exp[2D_{KL}(Z_2||Z_2^G)] \\ & + N(Z_{12})\exp[2D_{KL}(Z_{12}||Z_{12}^G)],\end{aligned} \tag{64}$$

which is exactly (14) for $m = 2$. Thus, we have verified the entropy power decomposition for the two-dimensional case.

References

D. Allaire and K. Willcox, A Variance-Based Sensitivity Index Function for Factor Prioritization, Reliability Engineering and System Safety, 107 (2012), 107–114.

D. Allaire, Q. He, J. Deyst, and K. Willcox, An Information-Theoretic Metric of System Complexity with Application to Engineering System Design, Journal of Mechanical Design, 134(10) (2012), 100906–1–10.

D. L. Allaire, Uncertainty Assessment of Complex Models with Application to Aviation Environmental Systems, Ph.D. Thesis, Massachusetts Institute of Technology, Cambridge, MA, 2009.

A. H. Ang and W. H. Tang, Probability Concepts in Engineering: Emphasis on Applications to Civil and Environmental Engineering, 2nd edition, John Wiley & Sons, Inc., Hoboken, NJ, 2007.

S. Becz, A. Pinto, L. E. Zeidner, R. Khire, A. Banaszuk, and H. M. Reeve, Design System for Managing Complexity in Aerospace Systems, 10th AIAA ATIO Conference, AIAA Paper 2010-9223, Fort Worth, TX, 2010.

M. Belfiore, Adaptive Vehicle Make: DARPA's Plan to Revolutionize Auto Manufacturing, Popular Mechanics, Jan. 26, (2012).

D. Braha and O. Maimon, The Design Process: Properties, Paradigms, and Structure, IEEE Transactions on Systems, Man and Cybernetics, Part A: Systems and Humans, 27(2) (1997), 146–166.

O. Brown and P. Eremenko, The Value Proposition for Fractionated Space Architectures, AIAA Space 2006, AIAA Paper 2006-7506, San Jose, CA, 2006.

T. R. Browning, J. J. Deyst, S. D. Eppinger, and D. E. Whitney, Adding Value in Product Development by Creating Information and Reducing Risk, IEEE Transactions on Engineering Management, 49(4) (2002), 443–458.

L. L. Campbell, Exponential Entropy as a Measure of Extent of a Distribution, Probability Theory and Related Fields, 5(3) (1966), 217–225.

T. M. Cover and J. A. Thomas, Elements of Information Theory, John Wiley & Sons, Inc., New York, NY, 1991.

C. M. Creveling, J. L. Slutsky, and D. Antis, Jr., Design for Six Sigma in Technology and Product Development, Prentice Hall, Upper Saddle River, NJ, 2003.

J. J. Deyst, The Application of Estimation Theory to Managing Risk in Product Developments, Proceedings of the 21st Digital Avionics Systems Conference, vol. 1, Irvine, CA, 2002.

N. Ebrahimi, E. Maasoumi, and E. S. Soofi, Ordering Univariate Distributions by Entropy and Variance, Journal of Econometrics, 90(2) (1999), 317–336.

P. Eremenko, Formal Model-Based Design & Manufacture: A Template for Managing Complexity in Large-Scale Cyber-Physical Systems, Conference on Systems Engineering Research, Atlanta, GA, 2013.

A. Haldar and S. Mahadevan, Probability, Reliability and Statistical Methods in Engineering Design, John Wiley & Sons, Inc., New York, NY, 2000.

G. A. Hazelrigg, Systems Engineering: An Approach to Information-Based Design, Prentice-Hall, Upper Saddle River, NJ, 1996.

Q. He, D. L. Allaire, J. J. Deyst, and K. E. Willcox, A Bayesian Framework for Uncertainty Quantification in the Design of Complex Systems, 12th AIAA ATIO/14th AIAA/ISSMO MAO Conference, AIAA Paper 2012-5479, Indianapolis, IN, 2012.

T. Homma and A. Saltelli, Importance Measures in Global Sensitivity Analysis of Nonlinear Models, Reliability Engineering & System Safety, 52(1) (1996), 1–17.

J. D. Irwin and R. M. Nelms, Basic Engineering Circuit Analysis, 8th edition, John Wiley & Sons, Inc., Hoboken, NJ, 2005.

K. C. Kapur and L. R. Lamberson, Reliability in Engineering Design, John Wiley & Sons, Inc., New York, NY, 1977.

A. Karl, Robust Design and Stochastics: Key Methods, Case Studies and Challenges, MDO Consortium Workshop, Stanford, CA, 2013.

M. C. Kennedy and A. O'Hagan, Bayesian Calibration of Computer Models, Journal of the Royal Statistical Society, Series B, 63(3) (2001), 425–464.

J. Kim and D. Wilemon, Sources and Assessment of Complexity in NPD Projects, R&D Management, 33(1) (2003), 15–30.

F. Knoll and T. Vogel, Design for Robustness, IABSE (International Association for Bridge and Structural Engineering), Zurich, Switzerland, 2009.

S. Kullback and R. A. Leibler, On Information and Sufficiency, The Annals of Mathematical Statistics, 22(1) (1951), 79–86.

Z. Lattmann, A. Nagel, J. Scott, K. Smyth, J. Ceisel, C. vanBuskirk, J. Porter, S. Neema, T. Bapty, D. Mavris, and J. Sztipanovits, Towards Automated Evaluation of Vehicle Dynamics in System-Level Designs, Proceedings of the ASME International Design Engineering Technical Conference & Computers and Information in Engineering Conference (IDETC/CIE 2012), Chicago, IL, 2012.

H. Liu, W. Chen, and A. Sudjianto, Relative Entropy Based Method for Probabilistic Sensitivity Analysis in Engineering Design, Journal of Mechanical Design, 128(2) (2006), 326–336.

D. Mukherjee and M. V. Ratnaparkhi, On the Functional Relationship Between Entropy and Variance with Related Applications, Communications in Statistics – Theory and Methods, 15(1) (1986), 291–311.

NASA, NASA Systems Engineering Handbook, NASA/SP-2007-6105 Rev1 edition, National Aeronautics and Space Administration, Washington, DC, 2007.

P. Nightingale, The Product-Process-Organisation Relationship in Complex Development Projects, Research Policy, 29(7-8) (2000), 913–930.

W. L. Oberkampf, S. M. DeLand, B. M. Rutherford, K. V. Diegert, and K. F. Alvin, Error and Uncertainty in Modeling and Simulation, Reliability Engineering and System Safety, 75 (2002), 333–357.

P. Y. Papalambros and D. J. Wilde, Principles of Optimal Design: Modeling and Computation, 2nd edition, Cambridge University Press, New York, NY, 2000.

C. J. Roy and W. L. Oberkampf, A Comprehensive Framework for Verification, Validation, and Uncertainty Quantification in Scientific Computing, Computer Methods in Applied Mechanics and Engineering, 200 (2011), 2131–2144.

A. Saltelli, K. Chan, and E. M. Scott, Sensitivity Analysis, John Wiley & Sons, Inc., New York, NY, 2000.

C. E. Shannon, A Mathematical Theory of Communication, The Bell System Technical Journal, 27 (1948), 379–423 and 623–656.

R. C. Smith, Uncertainty Quantification: Theory, Implementation, and Applications, SIAM Computational Science & Engineering, Philadelphia, PA, 2014.

I. M. Sobol', Sensitivity Estimates for Nonlinear Mathematical Models, Mathematical Modeling and Computational Experiment, 1(4) (1993), 407–414.

I. M. Sobol', Global Sensitivity Indices for Nonlinear Mathematical Models and Their Monte Carlo Estimates, Mathematics and Computers in Simulation, 55 (2001), 271–280.

I. M. Sobol', Theorems and Examples on High Dimensional Model Representation, Reliability Engineering & System Safety, 79(2) (2003), 187–193.

N. P. Suh, The Principles of Design, Oxford University Press, New York, NY, 1990.

H. Takeda, P. Veerkamp, T. Tomiyama, and H. Yoshikawa, Modeling Design Processes, AI Magazine, 11(4) (1990), 37–48.

S. Thomke and D. E. Bell, Sequential Testing in Product Development, Management Science, 47(2) (2001), 308–323.

G. Warwick, F-35 JSF – Too Complicated?, Aviation Week, Mar. 26, (2010).

List of Tables

Table I: Best achievable uncertainty mitigation results given individual budgets for cost and uncertainty. Entries in red denote budget violations.

Active constraint	var (Y)	$C(Y)$	$P(Y < 300\,\mathrm{Hz})$	Cost
Complexity	1378	150	13.4%	8.8
Risk	1055	132	10%	14.8
Cost	780	114	6.4%	20

Table II: Local sensitivity predictions for the change in mean and standard deviation (SD) of each factor required to reduce risk to 10%

Component	Change mean only		Change SD only	
	$\Delta\mu_{X_i}$	Nominal value	$\Delta\sigma_{X_i}$	Tolerance
Resistor	$-3.4\,\Omega$	$R = 96.6\,\Omega$	$-8.4\,\Omega$	N/A
Capacitor	$-0.16\,\mu$F	$C = 4.54\,\mu$F	$-0.17\,\mu$F	$C_{\text{tol}} = \pm 14.4\%$

Table III: Uncertainty and cost estimates associated with various design options. Entries in red denote budget violations.

Option	$R\,(\Omega)$	R_{tol}	$C\,(\mu\text{F})$	C_{tol}	$\text{var}\,(Y)$	$C(Y)$	$P(Y < 300\,\text{Hz})$	Cost
Nominal	100	$\pm 10\%$	4.7	$\pm 20\%$	2015	181	18.6%	N/A
A	82	$\pm 10\%$	4.7	$\pm 20\%$	2997	221	0%	5
B	100	$\pm 10\%$	3.9	$\pm 20\%$	2927	218	0%	5
C	100	$\pm 1\%$	4.7	$\pm 20\%$	1627	154	18.1%	13.2
D	100	$\pm 10\%$	4.7	$\pm 10\%$	788	115	7.1%	22.5

List of Figures

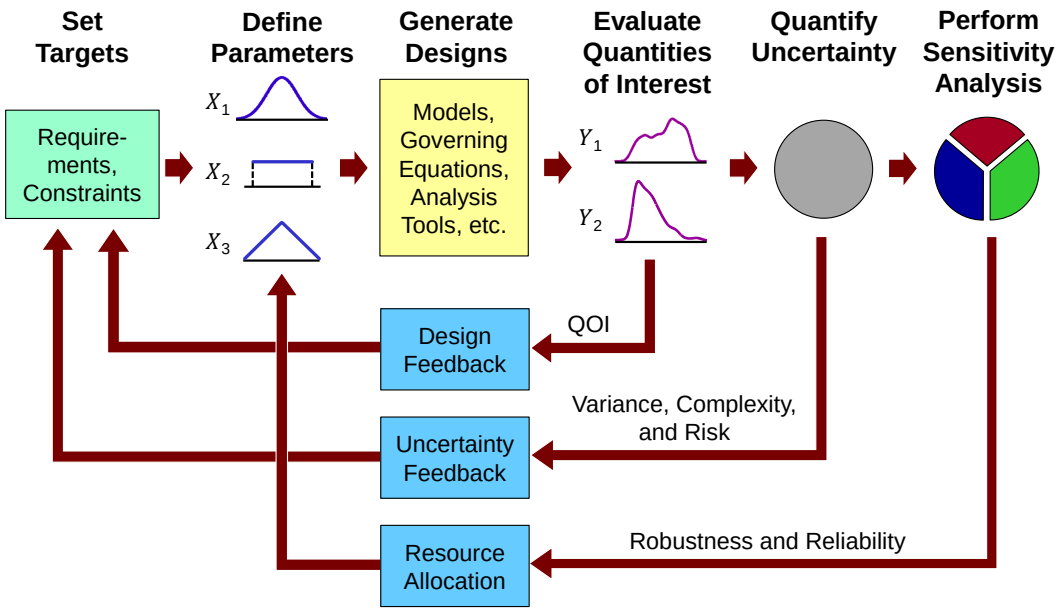

Figure 1: Schematic of the Bayesian system design framework

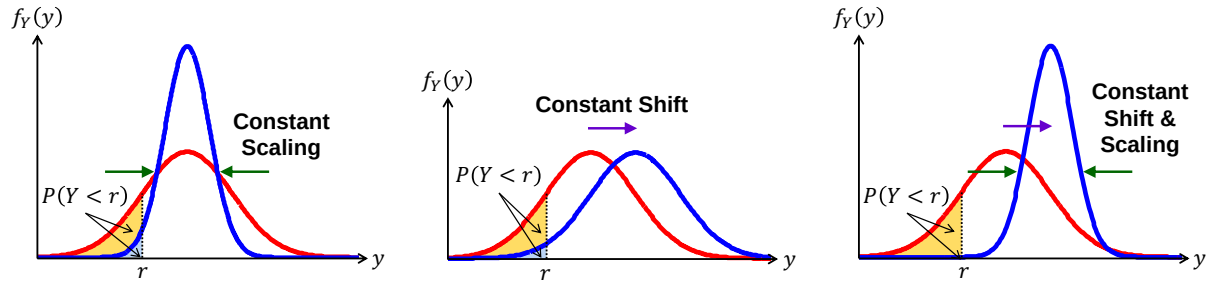

(a) Design for robustness (b) Design for reliability (c) Design for robustness and reliability

Figure 2: Schematics of design for robustness and reliability. Red and blue probability densities represent initial and updated estimates of $f_Y(y)$, respectively. Dashed line indicates the location of the requirement r. Shaded portions denote regions of failure in which the requirement is not satisfied.

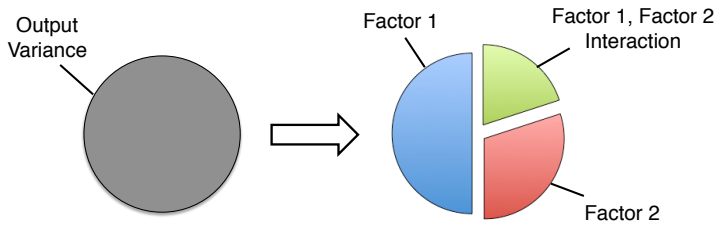

Figure 3: Apportionment of output variance in GSA [Allaire, 2009, Figure 3-1]

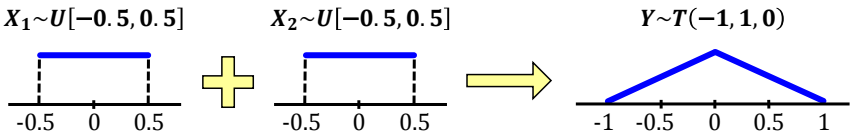

(a) Case 1: Example with $\zeta_1 > 1$ and $\zeta_2 > 1$

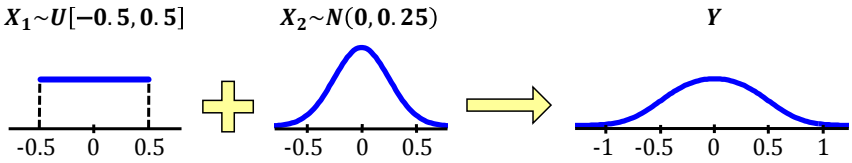

(b) Case 2: Example with $\zeta_1 > 1$ and $\zeta_2 < 1$

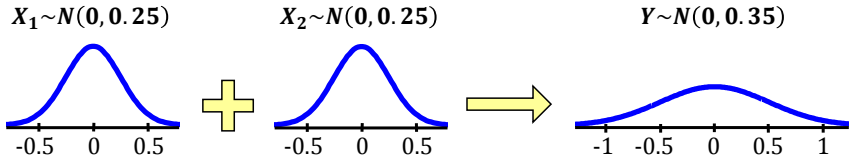

(c) Case 3: Example with $\zeta_1 = \zeta_2 = 1$

Figure 4: Examples of $Y = X_1 + X_2$ with increase, decrease, and no change in Gaussianity between the design parameters and QOI

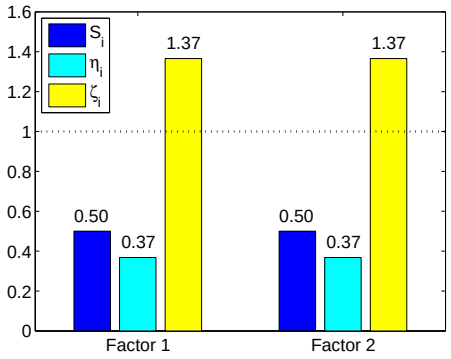

(a) Case 1: $X_1, X_2 \sim \mathcal{U}[-0.5, 0.5]$

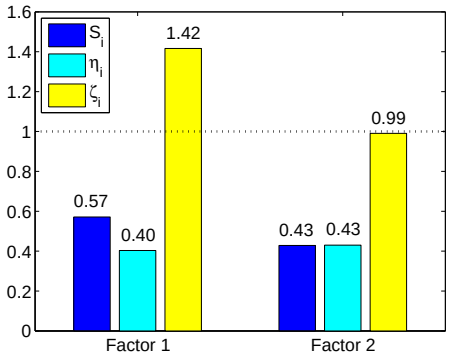

(b) Case 2: $X_1 \sim \mathcal{U}[-0.5, 0.5]$, $X_2 \sim \mathcal{N}(0, 0.25)$

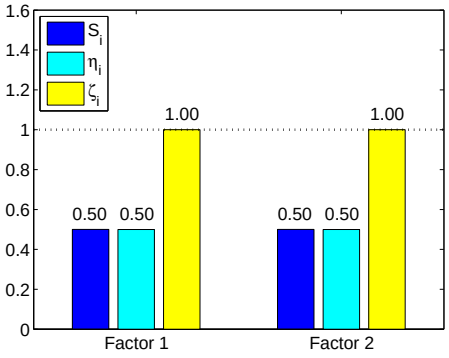

(c) Case 3: $X_1, X_2 \sim \mathcal{N}(0, 0.25)$

Figure 5: Sensitivity indices S_i, η_i, and ζ_i for three examples of $Y = X_1 + X_2$. For each factor, S_i equals the product of η_i and ζ_i.

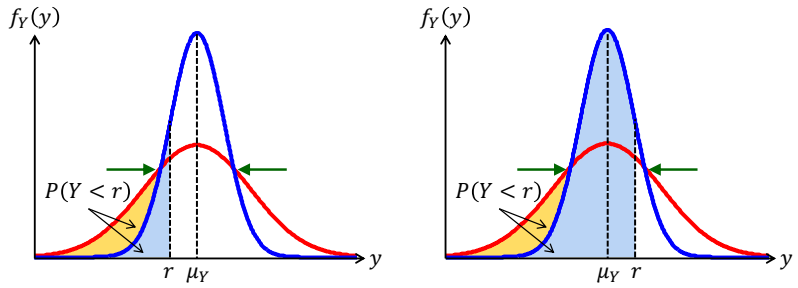

(a) $\mu_Y - r > 0$ (b) $\mu_Y - r < 0$

Figure 6: The relative locations of r and μ_Y greatly impact the change in risk associated with a decrease in σ_Y. Moving from the red probability density to the blue, $P(Y < r)$ decreases if $\mu_Y - r > 0$, and increases if $\mu_Y - r < 0$.

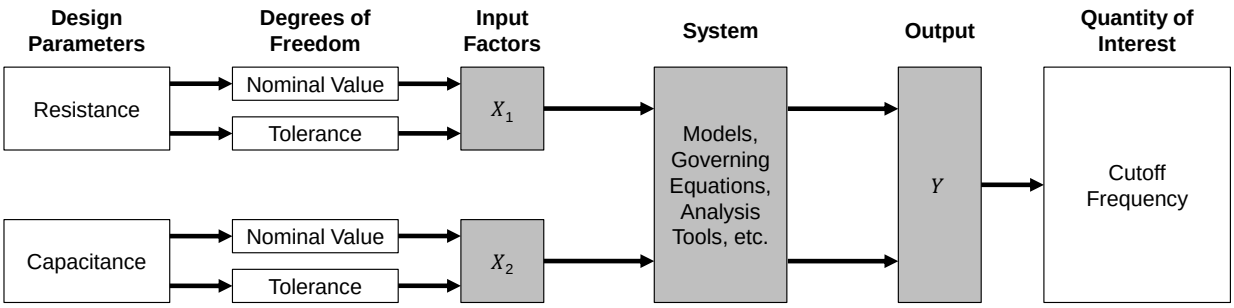

Figure 7: Block diagram of the circuit system

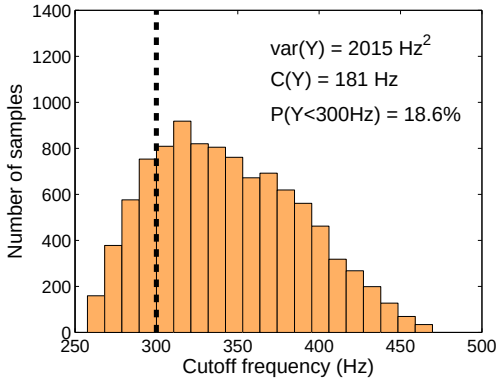

Figure 8: Histogram of cutoff frequency generated using 10,000 MC samples (dashed black line indicates the required cutoff frequency of 300 Hz)

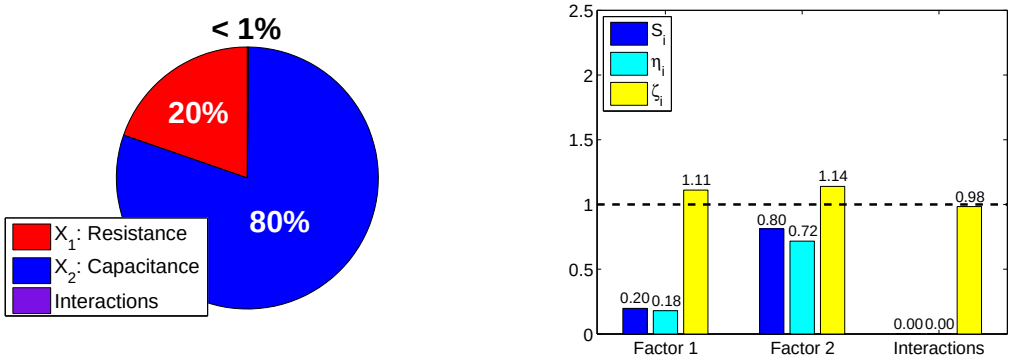

(a) Main effect sensitivity indices

(b) Entropy power sensitivity indices

Figure 9: Variance and entropy power sensitivity analysis results for the R-C circuit

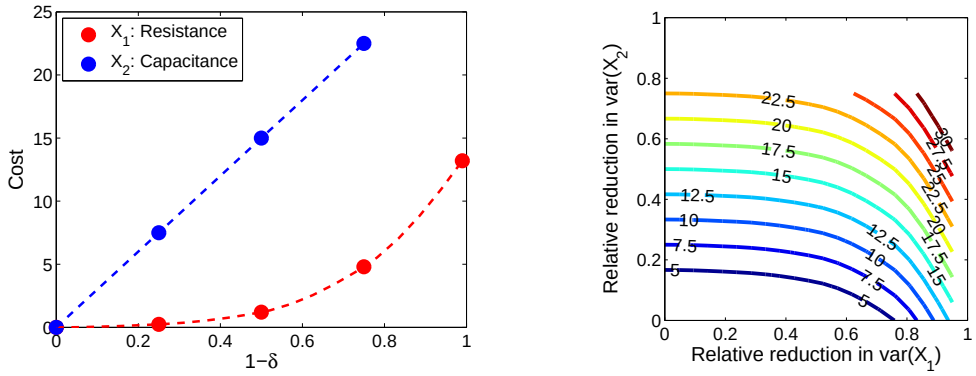

(a) Cost of reducing variance of X_1 or X_2

(b) Lines of constant cost

Figure 10: Notional cost associated with a $100(1-\delta)\%$ reduction in the variance of X_1 or X_2

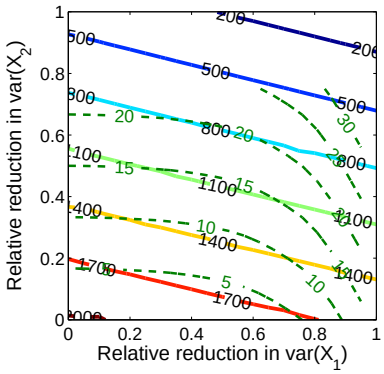

(a) Lines of constant variance and cost

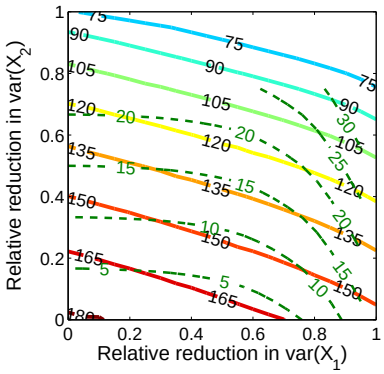

(b) Lines of constant complexity and cost

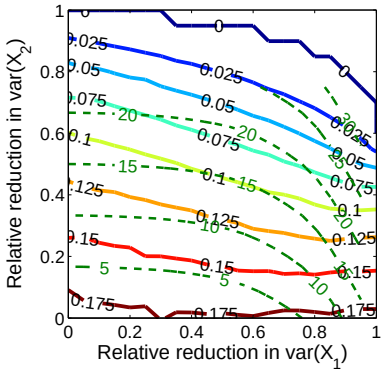

(c) Lines of constant risk and cost

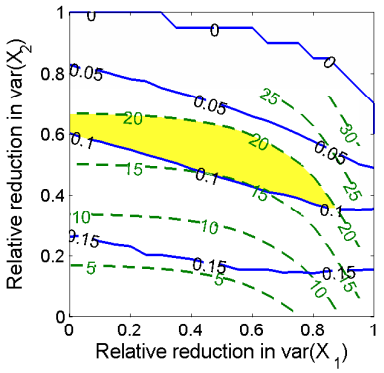

(d) Region in which all design budgets are satisfied

Figure 11: Contours for variance, complexity, and risk corresponding to reductions in factor variance (solid colored lines) overlaid with contours for cost of implementation (dashed green lines)

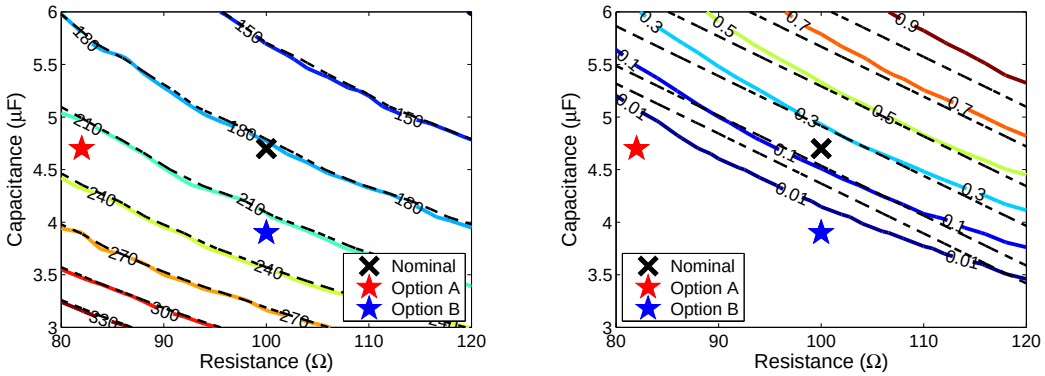

(a) Lines of constant complexity

(b) Lines of constant risk

Figure 12: Uncertainty contours for variations in resistance and capacitance, generated from 10,000 MC simulations (solid colored lines) or approximated using local sensitivity analysis results (dashed black lines)

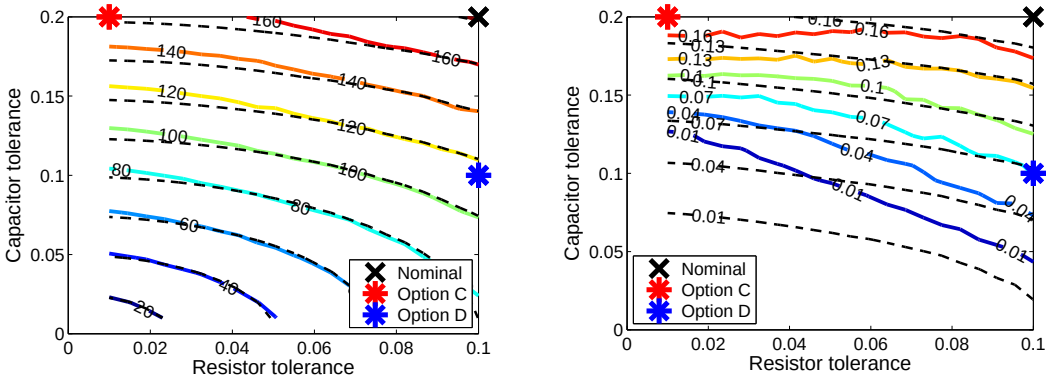

(a) Lines of constant complexity

(b) Lines of constant risk

Figure 13: Uncertainty contours for variations in resistor and capacitor tolerance

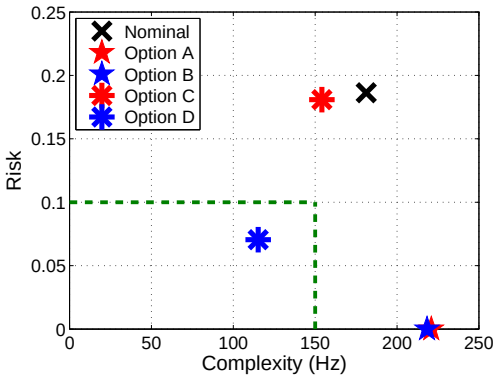

Figure 14: Tradeoffs in complexity and risk for various design options. Dashed green lines bound region where both complexity and risk constraints are satisfied.